Simulations of bubble division in the flow of a foam past an obstacle in a narrow channel

S.J. Cox[a]

[a]*Department of Mathematics, Aberystwyth University, SY23 3BZ, UK.*

Abstract

When foams flow through porous media, the interaction of the lamellae with the walls of the channels leads to changes in the bubble size distribution. We predict these changes using Surface Evolver simulations of simple foam structures subject to bubble creation via lamella division. We use a model porous medium consisting of a disc in a straight channel. The position of the disc within the channel is shown to significantly affect the final polydispersity of the foam, with a slightly off-centre disc giving the highest polydispersity. We also find that after repeated passes of the foam through the channel, the process of bubble division eventually ceases, leaving a foam with an average bubble area slightly larger than the disc size.

Keywords: foam generation; bubble division; porous media; simulation;

1. Introduction

Aqueous foams have many applications. The examples of improved oil recovery and soil remediation are typified by the flow of foam through a porous medium, in which it is unlikely that the distribution of bubble sizes remains constant in time because of the interaction of the foam lamellae with the tortuous channels found in, for example, oil-bearing rock. In particular, bubbles much larger than the pore size are unlikely to survive intact as a foam passes through a medium of given porosity, raising the following question: given an initial bubble size distribution and some details about the porosity of the medium, is it possible to predict how foam flow within the medium changes the bubble size distribution?

We attempt to answer this question here by considering a particularly simple two-dimensional (2D) porous medium, consisting of a narrow channel defined by very few geometrical parameters, two simple initial bubble size distributions, and very slow motion. We choose a simple channel shape to try and extract something fundamental about flows such as these, rather than trying to explain any particular situation. We choose to work in 2D because it is possible to see
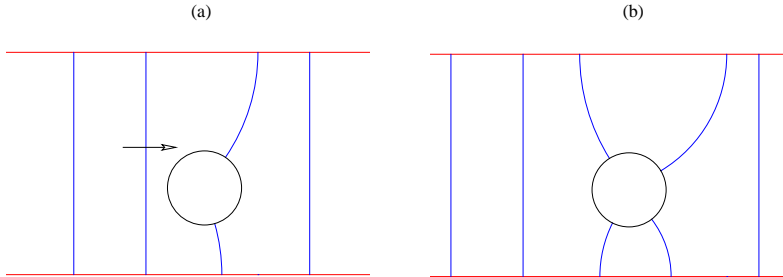

Figure 1: Two instants in time during the motion (from left to right) of a train of bubbles through a parallel-sided channel in which there is a circular obstacle. This is the initial configuration of the monodisperse foam considered here. (a) Before the division event, all bubbles have equal volume and all lamellae span the width of the channel. (b) When a lamella touches the obstacle, it divides a bubble into two pieces, and increases the total number of bubbles by one. (Note that another lamella has appeared at the left of the image.)

clearly what shapes the lamellae take and because the simulations are relatively quick; moreover, it has been shown in the past [1] that 2D theory, simulations and experiments can say something useful about real, three-dimensional foams. Finally, by simulating motion at the scale of individual lamellae, we can take advantage of the well-defined local geometry found in equilibrium dry foams to generate highly accurate, if idealized, results. This local geometry is given by what are known as Plateau's laws [1]: lamellae meet three-fold at angles of $120°$ and a lamella meets a solid wall at $90°$. In addition, the Laplace-Young law implies that each lamella is an arc of a circle.

We also try to determine whether, for fixed channel geometry, the process of lamella generation through bubble division [2], due to interaction with the channel walls, continues indefinitely, or, for a given channel, does the bubble size distribution saturate even though the foam continues to flow, and topological changes [3] continue to occur? Even at low flow-rates, we find that bubble division occurs due to purely geometrical effects.

2. Method

We ignore diffusion-driven coarsening and rupture due to e.g. lamella thinning under gravity. Instead, we assume that changes in bubble size occur only when a lamella hits something part-way along its length (figure 1), and the gas contained in the bubble is split into two parts (above and below the obstacle).

We use quasi-static simulations in Surface Evolver [4], assuming that changes in topology and bubble-size (caused by division) occur more quickly than the time-scale set by the gas (foam) flow-rate.

The foam is confined within a straight channel of length $L = 1$ and width H in which is placed a circular disc of radius R with its centre a distance y_0 from the lower wall. This is reminiscent of the geometry illustrated in [5] as a paradigm for bubble division. The initial foam structure is a bamboo foam of

2

ten bubbles in which each bubble touches both walls (see figure 1(a)). Except for those adjacent to the obstacle, all bubbles are initially rectangular. The channel is periodic in the direction of motion, so that bubbles moving out of the channel to the right re-enter on the left.

Unless stated otherwise, we take $H = 0.3$ and $R = 0.05$. We concentrate on two different initial conditions with respect to the bubble areas A, characterized by the normalized second moment of the area distribution:

$$\mu_2(A) = \frac{\overline{A^2}}{\overline{A}^2} - 1, \tag{1}$$

where the bar denotes an average over the foam. Either all bubbles have the same area (monodisperse, $\mu_2(A) = 0$) or we impose a range of areas (polydisperse). In the latter case, bubbles areas are varied at random by up to 50% of the monodisperse value, using the same seed each time to give a value of $\mu_2(A) = 0.0463$.

At each iteration, a region is defined from the upstream end of the channel to one of the lamellae (or, later, a line of lamellae, chosen far upstream of the disc) and the area of this region is increased by $dA = 1 \times 10^{-3}$ to move the foam downstream [6]. We perform this movement in ten small steps, interspersed with a few energy minimization steps, to avoid numerical problems. Then we define one *cycle* of the foam through the channel to consist of $(LH - \pi R^2)/dA \approx 300$ iterations. Each iteration includes convergence (to 16 decimal places) to a minimum of surface energy (total bubble perimeter). At each minimization step we check for lamellae overlapping the obstacle, in which case we split the lamella into two parts and the adjacent bubble into two regions, assigning target areas equal to the different values resulting from the overlap. Different configurations during which division occurs are shown in figure 2. Further, within the iteration we periodically check for short edges, performing T1 topological changes when these shrink below a length of $l_c = 8 \times 10^{-3}$, corresponding to a liquid fraction of about 10^{-5} [7]. We therefore neglect any possible dependence on liquid fraction, which of course may be important.

Each simulation is run until either the line-length (energy) of the structure appears periodic or, failing that (even at a steady-state of area distribution the energy does not always settle down to a repeated cycle, since T1 topological changes continue to occur), the second moment of the area distribution has not changed for more than eight cycles of the foam through the channel [8].

3. Results

If the disc is placed in the centre of the channel (i.e. $y_0/H = 0.5$, figure 3(a)) each bubble of the bamboo foam is split into two as it passes the disc, generating a foam of 20 bubbles. No further divisions occur and the simulation can then terminate. In the monodisperse case this gives a two-layer, or staircase, foam. Due to symmetry-breaking of the foam structure downstream of the disc, later divisions do not lead to equal area bubbles and the staircase structure is therefore non-uniform.

3

t = 122

t = 253

t = 317

t = 799
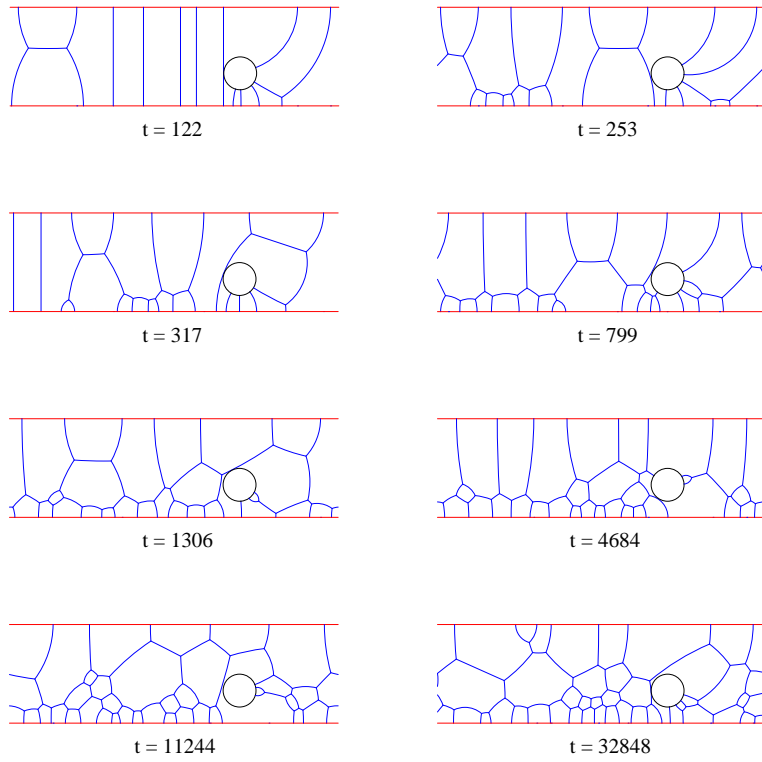
t = 1306

t = 4684

t = 11244

t = 32848

Figure 2: Different arrangements of lamellae just before division occurs, labelled by the number of iterations. In general, either large bubbles that span the width of the channel or severely curved lamellae lead to division. The images are taken from a simulation with $y_0/H = 0.33$ and an initially polydisperse foam structure.
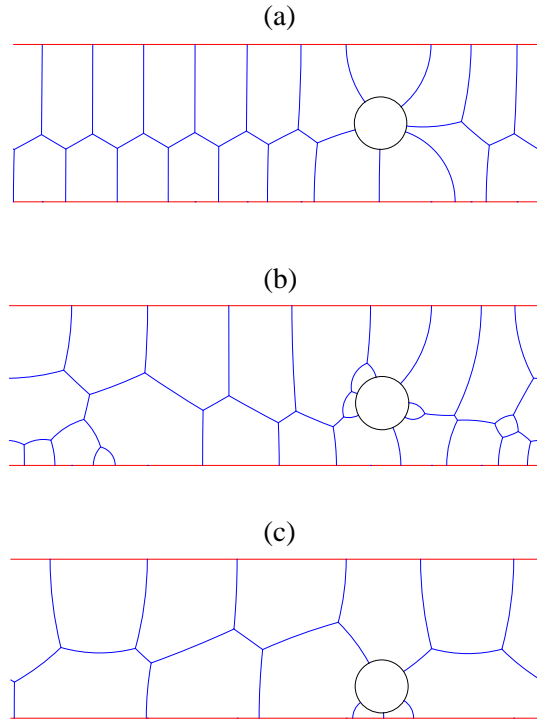
4

Figure 3: Examples of foams generated by the division process from an initially monodisperse foam. (a) $y_0/H = 0.50$: with the disc in the centre of the channel, a non-uniform staircase structure is formed. (b) $y_0/H = 0.39$: with the disc slightly off-centre, small bubbles are formed around the obstacle; they are not trapped between the obstacle and the wall, but move downstream and return to the obstacle from upstream, leading to many cycles of flow before the area distribution becomes stationary. (c) $y_0/H = 0.20$: when the disc is close to the wall, small bubbles are formed and then trapped.

For the division process to continue for longer, we therefore need to introduce asymmetry by placing the disc off-centre. By symmetry we need only consider $y_0/H \leq 0.5$. Then the division process introduces a greater disparity in size between the bubbles passing over the disc and those passing beneath it. The small bubbles that are formed are necessarily beneath the disc. For small y_0/H, it is possible that these small bubbles become trapped between the edge of the disc and the wall of the channel (figure 3(c)). This is the bubble-scale manifestation of the foam's yield stress, i.e. it is what makes it difficult to push foam through tortuous channels.

If these small bubbles poke out upstream of the leading edge of the disc, they cause the following bubbles to move up and over the obstacle (as in figure 3(c)) through a succession of T1 events. For example, at the smallest value used, $y_0/H = 0.2$, two bubbles are sufficient to fill the gap beneath the disc, and then bubble division stops with twelve bubbles and low area dispersity.

However, when these small bubbles do not poke out upstream, further division is likely to occur (figure 3(b)), leading to higher area dispersity. Sometimes the small bubbles are swept out from beneath the obstacle, which allows more cycles of bubble division to occur (as in figure 3(b)), and this leads to the longest simulations, and most polydisperse foams.

Figure 4 shows data from two simulations, one monodisperse and one polydisperse, with $y_0/H = 0.4$ (cf. figure 3(b)). In the monodisperse case one bubble never divides even though the process continues for about 16 cycles. The polydisperse simulation finishes more rapidly, after only four cycles. In both cases the area of the smallest bubble is a small fraction of its initial area, the average area decreases monotonically, and the second moment of area is non-monotonic: it mostly increases, with occasional decreases.

In figure 5(a) we show the number of cycles (equivalent to time) beyond which no further divisions occur, that is, the time at which the foam first reaches its final value of $\mu_2(A)$, as the gap between the disc and the wall changes. As described above, this time is longest when the disc is off-centre but not too close to the wall. For $y_0/H = 0.5$ the stopping time is exactly one cycle, and this is stable over a small range of y_0, irrespective of the initial polydispersity. For small y_0, bubbles get trapped easily, and the process of bubble division can stop quickly. At intermediate y_0/H the effect of initial polydispersity is greatest, and the time for the division process to cease can vary significantly between foams of different polydispersity.

Figure 5(a) also shows that the final value of $\mu_2(A)$ behaves similarly: that is, it is dependent on the number of divisions, which increases with the time for which the simulation runs. Only for $y_0/H = 0.5$, with the disc in the centre of the channel, does the final value of polydispersity reflect the initial value, since so few divisions occur. Figure 5(b) suggests that the process of bubble division ends when the average bubble area is close to the area of the obstacle, at least for this obstacle size.

Figure 6(a) shows more clearly the effect of initial polydispersity in the case where there is the largest disparity in saturation time in figure 5(a), that is, $y_0/H = 0.33$. The results of simulations at six intermediate values of the initial
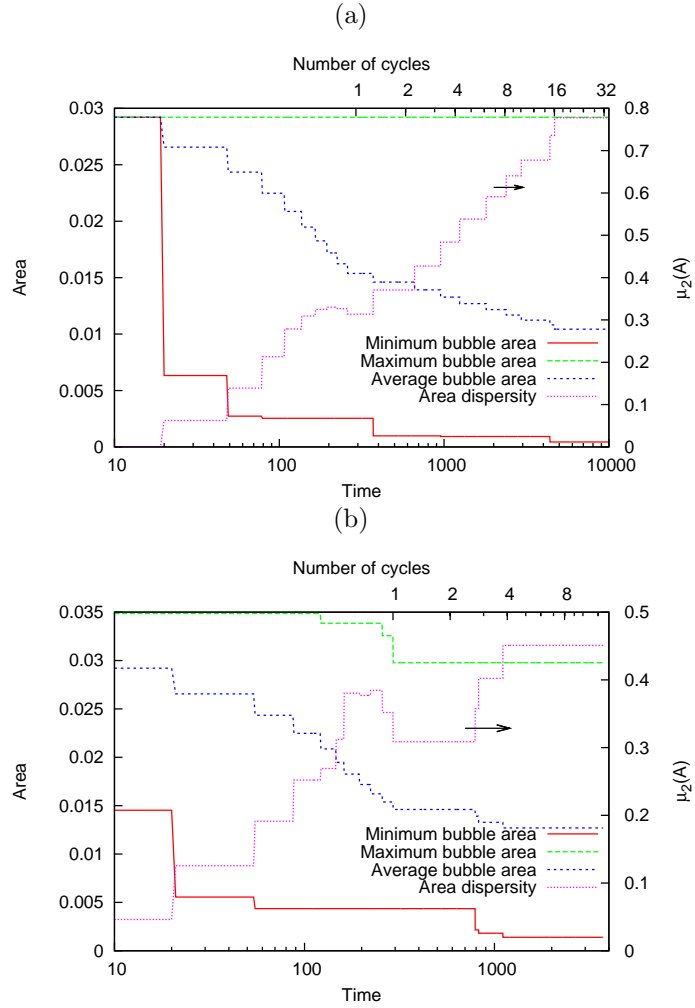
6

(a)

(b)

Figure 4: (a) An example of the evolution of the area distribution starting from a monodisperse foam in the case $y_0/H = 0.40$. We plot the maximum and minimum bubble areas, the average bubble area, and (on the right-hand axis) the second moment of the area distribution (area dispersity). (b) Same data for an initially polydisperse foam with $y_0/H = 0.39$. This polydisperse simulation is unusual in that the number of divisions saturates before the monodisperse simulation with the same value of y_0.
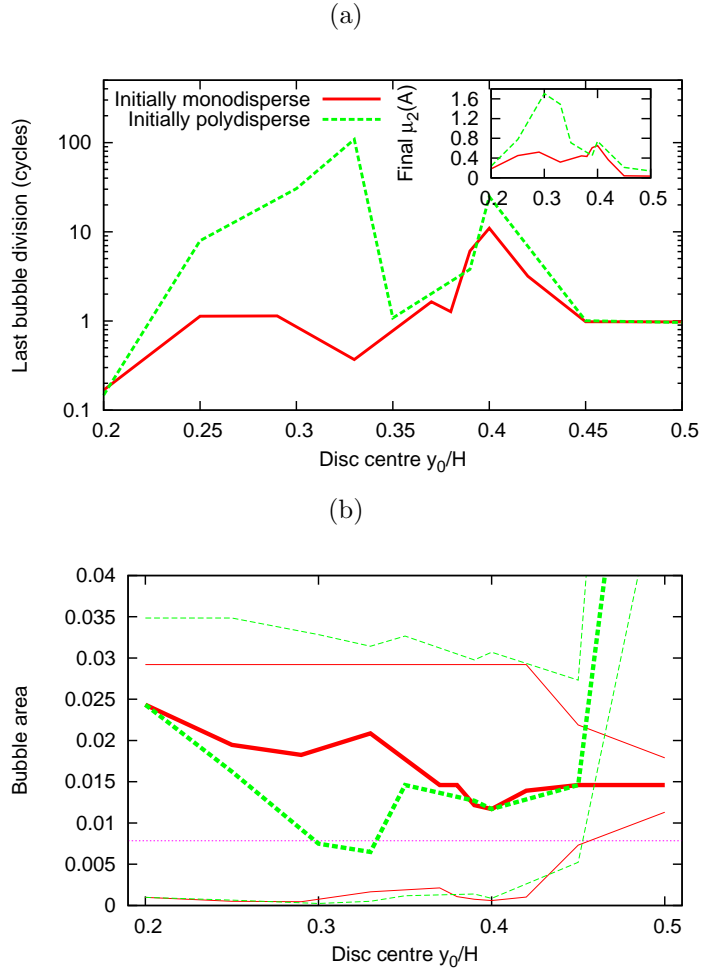
7

(a)

(b)

Figure 5: (a) The time taken for the area distribution to saturate depends strongly, and non-linearly, on the position of the disc. Note the log scale for the number of cycles, indicating that when the disc is off-centre, the polydisperse foam often takes much longer to saturate. The inset shows the final value of the area polydispersity ($\mu_2(A)$), which is closely related. (b) The average bubble area (thick lines) after saturation is almost constant, and slightly greater than the disc area (horizontal line). Note that the values for the initially polydisperse foam with $y_0/H = 0.5$ lie off the graph; the minimum and maximum bubble areas, shown as thin lines, are broadly similar in all other cases.

8

polydispersity show that, for this value of y_0/H, the number of cycles required for the lamella generation process to saturate increases (roughly exponentially) with the initial polydispersity. In particular, this indicates that the differences evident in figure 5 are systematic rather than random.

A disc radius of $R = 0.05$ is optimal in terms of generating foam for fixed centre position $y_0/H = 0.4$: figure 6(b) shows that all other values of R lead to rapid saturation, within one to two cycles. (Note now that a cycle takes a different number of iterations for different R, and that the bubble size changes slightly.) At smaller R, the disc is insufficient to make much difference to the flow after the first cycle, while for larger R small bubbles are trapped between the disc and the channel wall and the remaining bubbles pass over the disc without dividing.

4. Conclusions

The distribution of bubble sizes that is generated when a foam flows through a porous medium is extremely difficult to predict. Even in the simple channel geometry studied here, varying the position of the obstacle or the initial distribution of bubble sizes can lead to order-of-magnitude differences in the time taken for the bubble size distribution to saturate. However, we do find that this distribution does always saturate.

We have been able to characterise the effect of changing the size and position of the obstacle in the channel: if it is large or small compared to the channel width, or close to the wall or close to the centre of the channel, it suppresses bubble division and leads to only minor changes in the bubble size distribution. On the other hand, with a disc with diameter one-third of the channel width, situated part way between the channel centre and the wall, a significant number of division events occur and the resulting foams are highly polydisperse.

Changing the initial number of bubbles or, broadly equivalently, changing the bubble size A relative to the channel width H, is something that should be pursued in the future. It may also be of interest to vary the liquid fraction (through the parameter l_c in the first instance). Increasing the number of discs in the channel and the number of bubbles (figure 7) should lead to a more realistic approximation to actual porous media, allowing questions such as how a foam chooses which channels to follow when presented with many choices [9]. It should also be possible to measure the pressure drop required to keep the foam flowing in such geometries.

As stated above we have neglected foam coarsening, yet if the flow rate of the foam was sufficiently slow, then the process of gas diffusion between the bubbles caused by differences in their pressure might play a role. The relevant dimensionless parameter is the ratio $\mu = \kappa H/dA$, where κ is the diffusion coefficient and dA is the advection parameter given above; the simulations above correspond to the limit $\mu = 0$. Adding gas diffusion to the simulations is achieved by, at the beginning of each iteration, calculating the product of pressure difference and length across each lamella and changing the bubble areas in proportion to the sum of this quantity around each bubble. We find that $\mu = 3$ corresponds
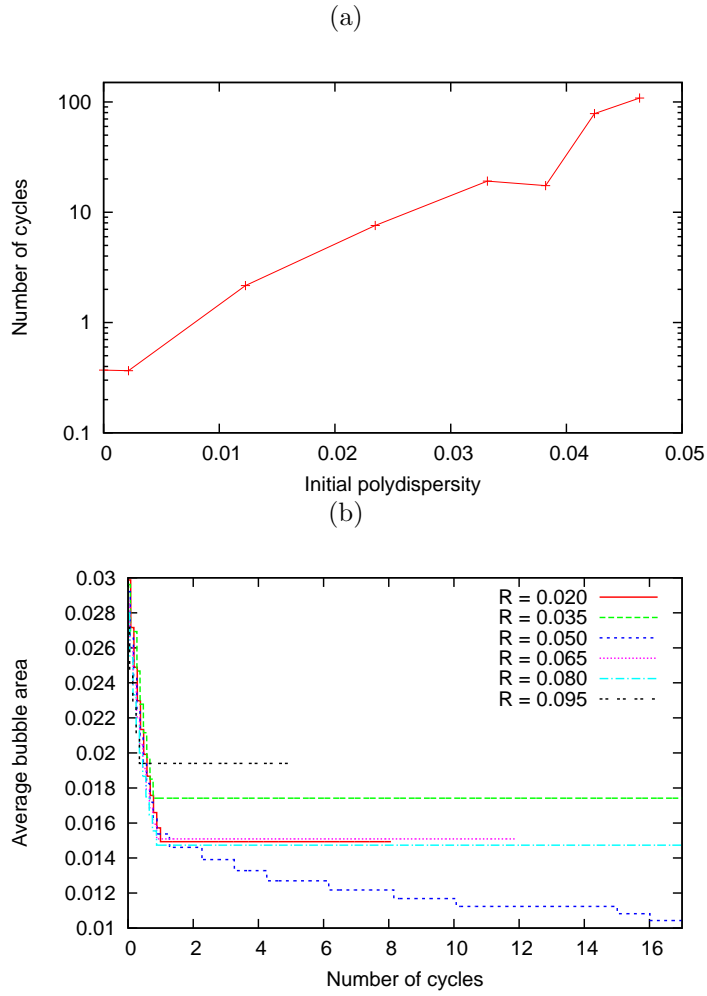
9

(a)

(b)

Figure 6: (a) The disc size and position are fixed at $R = 0.050$ and $y_0/H = 0.33$, corresponding to the greatest difference in stopping time in figure 5(a), and the initial polydispersity $(\mu_2(A))$ of the foam is varied. The number of cycles required for the foam generation process to saturate increases almost monotonically with the polydispersity. (b) The centre of the disc is fixed at $y_0/H = 0.4$ and its radius varied. In every case the average bubble area decreases; the smallest bubbles are generated for $R = 0.050$, which takes the longest time to saturate.
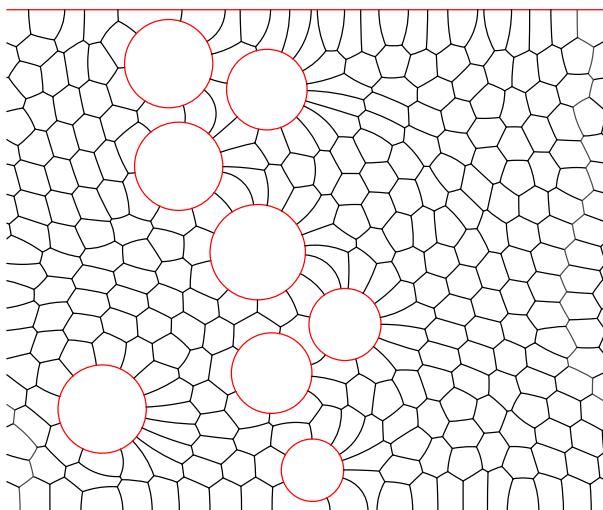
10

Figure 7: Surface Evolver simulation of monodisperse foam flowing through a porous medium consisting of eight discs in a straight channel. Is it possible to predict which channels between the discs permit flow?

to rapid coarsening: the lamella curvatures (or, equivalently, the pressure differences between bubbles) generated by the presence of the disc (cf. figure 1(b)) lead in this case to each bubble disappearing when it passes above or below the disc. The neighbouring bubbles grow, until only one or two bubbles remain in the channel, therefore making the foam ineffective as a displacement fluid [10]. Even $\mu = 0.3$ is sufficiently large that after two or three cycles only a few bubbles remain. In the future, it would be interesting to determine the value of μ at which bubbles are generated by division at the same rate that they are lost through diffusion-driven coarsening.

Acknowledgements

References

[1] I. Cantat, S. Cohen-Addad, F. Elias, F. Graner, R. Höhler, O. Pitois, F. Rouyer, A. Saint-Jalmes, Foams - structure and dynamics, OUP, Ox-

ford, 2013.

[2] W. Rossen, Foams in Enhanced Oil Recovery, in: Foams: Theory, Measurements and Applications, Marcel Dekker, New York, 1996, pp. 413–464.

[3] D. Weaire, N. Rivier, Soap, cells and statistics–random patterns in two dimensions, Contemp. Phys. **25** (1984) 59–99.

[4] K. Brakke, The Surface Evolver, Exp. Math. **1** (1992) 141–165.

[5] T. Ransohoff, C. Radke, Mechanisms of foam generation in glass-bead packs, SPE Reservoir Engineering **3** (1988) 573–585.

[6] S. Cox, B. Dollet, F. Graner, Foam flow around an obstacle: simulations of obstacle-wall interaction, Rheol. Acta. **45** (2006) 403–410.

[7] C. Raufaste, B. Dollet, S. Cox, Y. Jiang, F. Graner, Yield drag in a two-dimensional foam flow around a circular obstacle: Effect of liquid fraction, Euro. Phys. J. E **23** (2007) 217–228.

[8] Example videos of the motion are available at http://users.aber.ac.uk/sxc/foam_movies.html.

[9] S. Jones, B. Dollet, Y. Meheust, S. Cox, I. Cantat, Structure-dependent mobility of a dry aqueous foam flowing along two parallel channels, Phys. Fluids **25** (2013) 063101.

[10] L. Nonnekes, S. Cox, W. Rossen, Effect of Gas Diffusion on Mobility of Foam for Enhanced Oil Recovery, Submitted to Transport in Porous Media.